# Numerical Study of the Fluid Flow and Temperature Distribution in a Non-transferred DC ARC Thermal Plasma Reactor

**Yudong Li and Ramana G. Reddy**

**Abstract** Numerical modeling of the thermal plasma process was carried out based on the thermal plasma reactor in our lab and confirmed using experimental data. The inlet boundary conditions of a non-transferred DC arc thermal plasma reactor were used in modeling the temperature and fluid flow distribution in the reactor. Different mesh grid sizes were used to confirm the model is independent of grid size. Temperature profile and gas flow distribution in the thermal plasma reactor were developed by the computational fluid dynamics (CFD) with ANSYS Fluent. The predicted temperatures are in good agreement with the experimentally measured temperatures in the reactor. The influence of plasma torch input power as well as the plasma gas flux on the temperature distribution was investigated using this model. The influence of power input and gas flow rate on temperature and velocity distributions are not independent. Generally, higher power input and lower gas flow rate will give rise to the temperature increase in the reactor.

**Keywords** Thermal plasma · Material plasma synthesis · Computational fluid dynamics · Arc jet flow · Plasma model

## Introduction

Thermal plasma processing (TPP) techniques [1] are widely used for spraying, coating, synthesis, sintering, extractive metallurgy and waste treatment. Due to its high energy content and high energy density, TPP brings large opportunities for materials processing. It has a lot of advantages in synthesizing materials, such as, enhanced kinetics because of plasma and gaseous state reactions, lower activation

Y. Li · R.G. Reddy (✉)
Department of Metallurgical and Materials Engineering,
The University of Alabama, Tuscaloosa, AL 35487, USA
e-mail: rreddy@eng.ua.edu



S. Wang et al. (eds.), *Applications of Process Engineering Principles in Materials Processing, Energy and Environmental Technologies*,
The Minerals, Metals & Materials Series, DOI 10.1007/978-3-319-51091-0_43

energy in the plasma state and high purity synthesizing because of its clean atmosphere. Moreover, the thermal plasma reactor (TPR) in our lab integrated a quench tube for shock quenching which will quench the product in a short amount of time forming nanoscale products. There are numerous reports on the production of high temperature ceramics [2, 3] and composites by TPP such as TiC nano-powders [4], TiC/TiN-Al(Ti) ultrafine composite powders [5], and SiC nano-powders [6]. Due to the high temperature and the set up of TPR in our lab, it is not possible to measure the gas flow and temperature distribution. However, the computational fluid dynamics (CFD) can be used as a powerful tool to investigate the flow pattern and heat transfer inside the TPR and to gain a better understanding of the physical phenomena of TPP.

Plasma jet flow is highly complex due to high temperature and high velocity. There are numerous investigations that have been done in modeling of the plasma spray process using CFD. Mashayak et al. has done CFD modeling of the thermal plasma process for waste treatment [7]. They used steady state incompressible Navier-Stokes equations with a standard $k$-$\varepsilon$ turbulence model to account for the fluid flow. Lorcet et al. has done the kinetics modeling with CFD of biomass gasification process using TPR [8]. Matveev et al. has done TPP modeling using CFD for coal gasification process using a hybrid plasma torch [9]. Fan et al. has investigated the effect of operation parameters [10], including current and flow rates of primary and secondary gas, on coating quality in plasma spray process. Mankelevich et al. did modeling of the dc arc jet process in CVD reactors [11], which is basically very similar to TPP, using a two-dimensional model. Williamson et al. has done modeling of the high-velocity and high-temperature plasma jet [12]. Agon et al. has developed a three-dimensional CFD model to investigate the thermophysical properties of gas mixture effect on fluid flow in a hybrid $H_2O$/Ar plasma jet flow process [13].

In this work, we developed a three-dimensional CFD model based on the DC arc TPR in our lab which described the fluid flow and gas-solid-liquid coupled heat transfer phenomenon in the TPP. The plasma inlet boundary conditions are approximated using the known DC arc torch input power and the torch gas flow rate. Experimental data of the temperature measured at different thermocouple places were used to justify the model. Using the velocity profile as well as the temperature distribution inside TPR, we are able to have better understanding of the material synthesis process.

## Experimental Method

The model used in this study was developed to study the thermal plasma synthesis system in our lab, which contains a water cooling system, plasma generating system (with a non-transferred PT-50C plasma torch in DC arc mode), particle feeding system, reactor chamber and temperature measurement system. Figure 1 shows the photo and schematic diagram of the TPR. The TPR mainly consists of three zones.

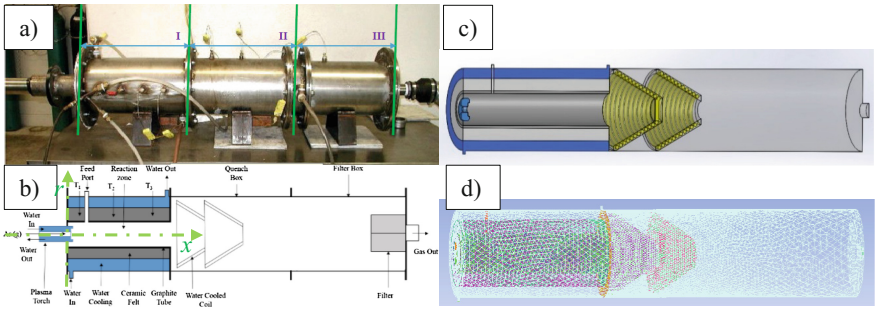


**Fig. 1** Photograph (**a**) and schematic diagram (**b**) of the TPR (**c**) and (**d**) are Geometry and one computational mesh used in this study, respectively

**Fig. 2** Temperature and velocity distribution at nozzle exit

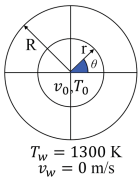


They are the reaction zone ($x$ = 0–450 mm), Zone **I**; the quenching zone ($x$ = 450–900 mm), Zone **II**; the filter zone ($x$ = 900–1350 mm), Zone **III**. Outer shell of the whole reactor is made of 316L stainless steel. Zone **I** consists of five parts: a plasma gun port for connecting a plasma gun, a powder feeding port, a water-cooling jack ($r$ = ±87–115 mm) with cooling water inlet port and outlet port, an insulation layer ($r$ = ±52–87 mm) and a graphite tube ($r$ = ±45–52 mm). Zone **II** and Zone **III** are basically two stainless steel chambers with two cone-shape water-cooled copper quench coils and a cloth filter, respectively.

## *Geometry and Computational Mesh*

The three-dimensional geometry and a representative computational mesh used in this work are shown in Fig. 2, which used same dimension parameters as the TPR to ensure geometrical similarity for modeling [14]. All features, including three layers as we mentioned above, at Zone **I** are included in the model. The cooling coil at the downstream of Zone **I** have large effect on fluid flow as well as heat transfer. So we considered the design of coils including a cap of the first coil which is in contrast to the previous study [15]. Connections of these two cone-shape cooling coils will not have a large influence and thus be reasonably neglected.

**Table 1** A summary of governing equations

| | | |
|---|---|---|
| Continuity | $\nabla \cdot (\rho \vec{v}) = 0$ | (1) |
| Momentum | $\nabla \cdot (\rho \vec{v}\vec{v}) = -\nabla p + \nabla \cdot \left(\mu[(\nabla \vec{v} + \nabla \vec{v}^T) - \frac{2}{3}\nabla \cdot \vec{v}I]\right) + \rho \vec{g}$ | (2) |
| Energy | $\nabla \cdot (\vec{v}(\rho E + p)) = \nabla \cdot (k \nabla T)$ | (3) |

## *Fluid Flow and Heat Transfer Model*

The fluid flow model in this work is assumed to be steady state turbulent flow. A standard $k$-$\varepsilon$ turbulence model was used to account for the turbulent flow [16, 17]. This model is capable of reproducing the overall flow field characteristics, including temperature, velocity and so on, with fair accuracy [17, 18]. Even though this model may not be suitable for all plasma jet flow conditions, it offers a practical compromise between simplicity and much more complicated models. Thus, considering our study is mainly focused on reproducing temperature and velocity profile, the standard $k$-$\varepsilon$ turbulence model is feasible for this study. Governing equations are summarized in Table 1 [19].

## *Boundary Conditions*

In this study, the flow of plasma from nozzle exit was defined by means of temperature and velocity. The profiles of temperature and velocity can be expressed by the following functions [12, 13, 20, 21]:

$$T = (T_0 - T_w)\left[1 - \left(\frac{r}{R}\right)^{n_T}\right] + T_w \tag{4}$$

$$v = v_0\left[1 - \left(\frac{r}{R}\right)^{n_v}\right] \tag{5}$$

where $T_0$ and $v_0$ are temperature and velocity at the center of nozzle exit respectively. $T_w$ is the temperature at the nozzle outlet wall. Considering the nozzle is made of copper, 1300 K is a reasonable approximation of $T_w$ [13]. Variables in Eqs. (4) and (5) are illustrated in Fig. 3.

Since we can only measure the plasma gun input power and the gas flow rate, we need to calculate for four variables, i.e. $T_0$, $n_T$, $v_0$ and $n_v$,based on Eqs. (4) and (5) respectively. We chose $n_v$ value of 1.688 and $n_T$ of 2.5 to solve for the value of $v_0$ and $T_0$ at different conditions in order to have a similar velocity distribution based on both experimental and numerical velocity distributions [13, 21, 22]. Calculated velocity distributions and temperature distribution are used as boundary conditions for the nozzle inlet by the User Defined Function (UDF). The UDF in this work also contains the customization of gas density considering materials properties used in this work are the same as those described in our previous work [5, 15, 23].

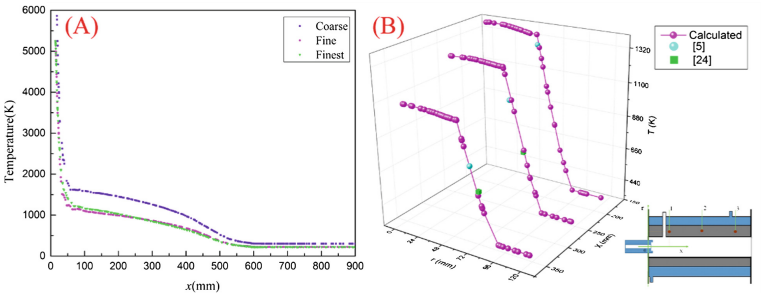


**Fig. 3** **A** is temperature profile on *x*-axis using different mesh and **B** is the validation of the model

## *Grid Independence Study*

In the grid independence study, we constructed three different computational meshes. They consist of 977,084 (coarse), 1,417,707 (fine) and 2,156,051 (finest) hexahedral cells respectively. In the grid independence study, the plasma power input was set to be 25 kW. Plasma gas flow rate was 6SCFM. Feeding gas flow rate was set to be 7.5 LPM. Temperature profiles along the axis of Zone I and Zone II downstream the nozzle exit of three different grid sizes are compared (at r = 0 mm, x = 0–900 mm, denoted as axis, also see Fig. 1). Results are shown in Fig. 3A. We can see that, using coarse grid will produce huge difference in the temperature distribution along x-axis. But, the fine grid agreed with the finest grid reasonably well. Due to the computational cost consideration, in this study we will use the fine mesh grid to achieve reasonable results reliability.

## *Model Verification*

Simulations were done using a plasma torch input power described previously [5, 24], i.e. 25.2 kW, for verification of the model. The radical temperature distributions at different thermocouple positions were calculated. The thermocouple positions are listed in Table 1.

The calculated temperature was compared with experimental data as shown in Fig. 3B and Table 2. There's not much difference between the calculated and experimentally measured temperature in previous works at different thermocouple points. So we can conclude that the model we developed in this work has a good agreement with experiment data and thus can be used for prediction of the temperature and velocity profile.

**Table 2** Thermocouple positions and comparison of calculated temperature with experimental measurements in previous work [5, 24]

| Thermocouple position | Radius ($r$/mm) | Length ($x$/mm) | $T_{Exp}$ | $T_{Calc}$ | References |
|---|---|---|---|---|---|
| 1 | 52.4 | 165.1 | 1273 | 1319.70 | [5] |
| 2 | 57.4 | 254.9 | 1023 | 1078.03 | |
| 3 | 62.4 | 342.9 | 773 | 771.22 | |
| 2′ | 70.0 | 255.0 | 698 | 725.05 | [24] |
| 3′ | 70.0 | 343.0 | 625 | 586.78 | |

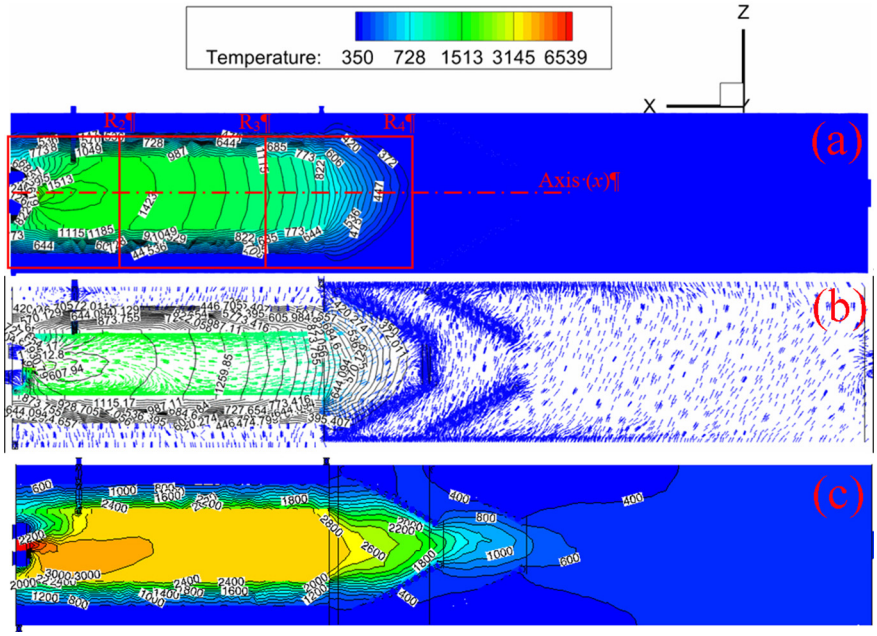


**Fig. 4** Temperature profile **a** and velocity vector distribution **b** of 25.2 kW and 6SCFM; **c** is the temperature distribution in the model without cap at the first coil [15]

## Results and Discussion

### *Temperature and Velocity Distribution*

Figure 4a, b shows the temperature distribution and velocity distribution of a power input of 25.2 kW and plasma gas flow rate of 6 SCFM along a center slice of the TPR. We can see that from the first quenching coil to the outlet at Zone III, the fluid flow and temperature distribution is almost uniform and do not vary much from those before the first cooling coil.

In comparing with previous work [15], this model includes a cap at the first coil which was omitted by previous work, shown in Fig. 4c. Comparing Fig. 4a, c, we can see that with a cap the temperature is lowered at Zone I. And the temperature calculated in this work is closer to what is measured experimentally than previous tests.

## *Plasma Input Power Effect*

Plasma input power (P) has a great effect on the synthesis process in TPR. With all other boundary conditions fixed as stated in the boundary condition section, at plasma gas flow rate of 6SCFM, the input power of 18.2, 22.4 and 25.2 kW were used in the calculation which is the same as the experimental operation parameters in previous work [5, 25]. The input power effect on temperature distribution was investigated as shown in Fig. 5A, B. As shown in Fig. 5, plasma power input has a large effect on the temperature distribution inside Zone I. The temperature will generally increase with the increasing power input. Zone I can be divided into three different sections, R2 ($T > 1500$ K), R3 ($1500\ K > T > 1000$ K) and R4 ($T < 1000$ K). As seen that with the power input increase, section R2 and R3 enlarged, which is good for high temperature favorable chemical reactions in material synthesizing.

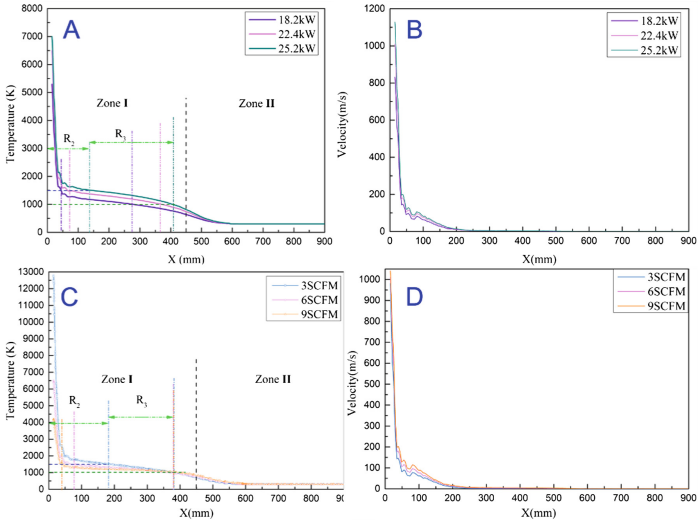


**Fig. 5** Temperature and velocity distribution on axis at different plasma power (**A**, **B**) and different plasma gas flow rates (**C**, **D**)

### *Plasma Gas Flow Rate Effect*

Plasma gas flow rate (or the plasma gun input gas flow rate, denoted as Q) turned out to be a very important factor influencing the material synthesis process in this study. However, to our knowledge, people have rarely studied the effect of plasma gas (argon gas in this study) flow rate. No work has been done considering the plasma gas flow rate effect both experimentally and numerically.

In this study, three different cases were calculated using different Q, 3SCFM, 6SCFM and 9SCFM. The power input in this study is fixed at 22.4 kW. After calculations were done of these three cases, temperature distributions on x-axis at different input power are plotted for comparison as shown in Fig. 5C, D.

Considering both axial temperature distributions, we can see that as the plasma gas flow rate decreased from 9SCFM to 3SCFM, section R2 is increasing while section R4 remains the same. Lower velocity may increase the residence time of particle inside the reactor which is good for vaporization of particles as well as reaction kinetics. Thus, we can conclude that, lower the plasma gas flow rate will increase the residence time and enhance the reaction kinetics due to the increasing of temperature.

## Conclusions

In this study, a numerical model was developed for thermal plasma reactor (TPR). The geometry used in this model was simplified based on the TPR from our lab. Different mesh grid sizes were used to confirm the model is independent of grid size. Data predicted by the model were compared with experimental data. The influence of plasma torch input power and plasma gas flow rate on the TPR was investigated using this model. The numerical results suggested that higher input power will result in higher temperature which is an advantage in producing materials which are high temperature favorable. The model also implied that plasma gas flow rate is a crucial factor that can influence the material synthesis process. Lower plasma gas flow rate is preferred considering both its temperature profile and velocity distribution. Though the modeling, we can see that the influence of power input and gas flow rate on temperature and velocity distribution is not independent but rather coupled. So in modeling the material synthesis in TPR, we should simultaneously consider the effects of both plasma power input as well as gas flow rate on temperature and velocity distributions.

**Acknowledgments** The authors are thankful for the financial support from National Science Foundation (NSF) agency (Grant No. DMR-1310072), American Cast Iron Pipe Company (ACIPCO) and The University of Alabama during the course of the current research project.

## References


1. M.I. Boulos, Thermal plasma processing. IEEE Trans. Plasma Sci. **19**(6), 1078–1089 (1991)
2. H.-C. Lee, S. Dhage, M.S. Akhtar, D.H. Kwak, W.J. Lee, C.-Y. Kim, O.-B. Yang, A simulation study on the direct carbothermal reduction of $SiO_2$ for Si metal. Curr. Appl. Phys. **10**(2), S218–S221 (2010)
3. N. Thakkar, R.G. Reddy, Thermal plasma production of B4C nanopowders. J. Manuf. Sci. Prod. **7**(2), 87–100 (2006)
4. L. Tong, R.G. Reddy, Synthesis of titanium carbide nano-powders by thermal plasma. Scr. Mater. **52**(12), 1253–1258 (2005)
5. S. Niyomwas, B. Wu, R.G. Reddy, *Synthesis of Fe-TiN Composites by Thermal Plasma Processing*. Ultrafine Grained Materials (as held at the 2000 TMS Annual Meeting, 2000), pp. 89–98
6. L. Tong, R.G. Reddy, Thermal plasma synthesis of SiC nano-powders/nano-fibers. Mater. Res. Bull. **41**(12), 2303–2310 (2006)
7. S.Y. Mashayak, *CFD Modeling of Plasma Thermal Reactor for Waste Treatment* (Purdue University West Lafayette, 2009)
8. H. Lorcet, D. Guenadou, C. Latge, M. Brothier, G. Mariaux, A. Vardelle, kinetics modeling of biomass gasification under thermal plasma conditions. Application to a refractory species: the methane. International symposium on plasma chemistry, Germany (Bochum, 2009)
9. I.B. Matveev, S. Serbin, Modeling of the coal gasification processes in a hybrid plasma torch. IEEE Trans. Plasma Sci. **35**(6), 1639–1647 (2007)
10. F. Qunbo, W. Lu, W. Fuchi, Modeling influence of basic operation parameters on plasma jet. J. Mater. Process. Technol **198**(1), 207–212
11. Y.A. Mankelevich, M. Ashfold, A. Orr-Ewing, Measurement and modeling of $Ar/H_2/CH_4$ arc jet discharge chemical vapor deposition reactors II: Modeling of the spatial dependence of expanded plasma parameters and species number densities. J. Appl. Phys. **102**(6), 063310 (2007)
12. R. Williamson, J. Fincke, D. Crawford, S. Snyder, W. Swank, D. Haggard, Entrainment in high-velocity, high-temperature plasma jets.: Part II: computational results and comparison to experiment. Int. J. Heat Mass Transf. **46**(22), 4215–4228 (2003)
13. N. Agon, J. Vierendeels, M. Hrabovský, A. Murphy, G. Van Oost, Interaction of a $H_2O$/AR plasma jet with nitrogen atmosphere: effect of the method for calculating thermophysical properties of the gas mixture on the flow field. Plasma Chem. Plasma Process. **35**(2), 365–386 (2015)
14. L. Yan, L. Yudong, Z. Ting'an, F. Naixiang, Research on the penetration depth in aluminum reduction cell with new type of anode and cathode structures. JOM **66**(7), 1202–1209 (2014)
15. Y. Li, R. Reddy, Experimental and numerical investigation of thermal plasma synthesis of silicon. J. Manuf. Sci. Prod. **15**(4), 345–354 (2015)
16. J. Ramshaw, C. Chang, Computational fluid dynamics modeling of multicomponent thermal plasmas. Plasma Chem. Plasma Process. **12**(3), 299–325 (1992)
17. C. Chang, J. Ramshaw, Numerical simulations of argon plasma jets flowing into cold air. Plasma Chem. Plasma Process. **13**(2), 189–209 (1993)
18. J. Fincke, C. Chang, W. Swank, D. Haggard, Entrainment and demixing in subsonic thermal plasma jets: comparison of measurements and predictions. Int. J. Heat Mass Transf. **37**(11), 1673–1682 (1994)
19. A. Fluent, Release 14.0, User Guide, Ansys, Inc., Lebanon, US (2011)
20. H. Lorcet, M. Brothier, D. Guenadou, C. Latge, A. Vardelle, Modeling bio-oil gasification by a plasma process. High Temp. Mater. Proc.: An Int. Q. High-Technol. Plasma Process. **14**(1–2) (2010)
21. M. Hrabovsky, V. Kopecký, V. Sember, T. Kavka, O. Chumak, M. Konrad, Properties of hybrid water/gas DC arc plasma torch. IEEE Trans. Plasma Sci. **34**(4), 1566–1575 (2006)

22. J. Fincke, D. Crawford, S. Snyder, W. Swank, D. Haggard, R. Williamson, Entrainment in high-velocity, high-temperature plasma jets. Part I: experimental results. Int. J. Heat Mass Transf. **46**(22), 4201–4213 (2003)
23. M. Ramachandran, R.G. Reddy, Thermal plasma synthesis of SiC. Advances in Manufacturing **1**(1), 50–61 (2013)
24. R.G. Reddy, L.V. Antony, Processing of SiC nano powders using thermal plasma technique. In *Proceedings of the International Conference on Nanotechnology: Scientific Challenges and Commercial Opportunities*, (Rhode Island, pp. 17–18, 2003)
25. L. Tong, R.G. Reddy, In situ synthesis of TiC-Al (Ti) nanocomposite powders by thermal plasma technology. Metall. Mater. Trans. B **37**(4), 531–539 (2006)